Oxidative and photochemical processes for the removal of galaxolide and tonalide from wastewater

Javier Santiago-Morales, María José Gómez, Sonia Herrera, Amadeo R. Fernández-Alba, Eloy García-Calvo, Roberto Rosal, Oxidative and photochemical processes for the removal of galaxolide and tonalide from wastewater, Water Research, Volume 46, Issue 14, Pages 4435-4447, 2012

https:/doi.org/10.1016/j.watres.2012.05.051

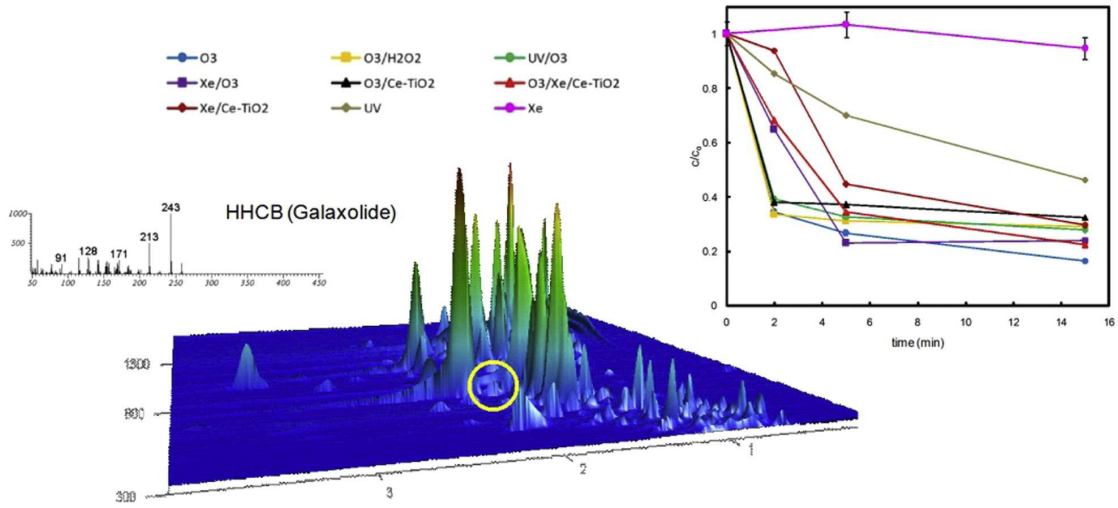

Oxidative and photochemical processes for the removal of galaxolide and tonalide from wastewater

Javier Santiago-Morales[1], María José Gómez[2], Sonia Herrera[2], Amadeo R. Fernández-Alba[2], Eloy García-Calvo[1,2], Roberto Rosal[1,2,*]

[1] Department of Chemical Engineering, University of Alcalá, 28871 Alcalá de Henares, Madrid, Spain

[2] Advanced Study Institute of Madrid, IMDEA Agua, Parque Científico Tecnológico, 28805 Alcalá de Henares, Madrid, Spain

* Corresponding author: roberto.rosal@uah.es

Abstract

Synthetic musks have been reported in wastewaters at concentrations as high as tens of micrograms per litre. The two most significant polycyclic musk fragrance compounds are 1,3,4,6,7,8-hexahydro-4,6,6,7,8,8-hexamethylcyclopenta(g)-2-benzopyran (HHCB, trade name galaxolide®) and 7-acetyl-1,1,3,4,4,6-hexamethyltetrahydronaphthalene (AHTN, trade name tonalide®). We report the result of several irradiation and advanced oxidation processes carried out on samples of the effluent of a wastewater treatment plant located in Alcalá de Henares, Madrid. Wastewater samples were pre-ozonated and spiked with 500 ng/L of tonalide or galaxolide in order to obtain final concentrations in the same order as the raw effluent. The treatments assayed were ozonation with and without the addition of hydrogen peroxide (O_3, O_3/H_2O_2), ultraviolet (254 nm low pressure mercury lamp) and xenon-arc visible light irradiation alone and in combination with ozone (UV, O_3/UV, Xe, O_3/Xe) and visible light photocatalytic oxidation using a Ce-doped titanium dioxide photocatalyst performed under continuous oxygen or ozone gas bubbling (O_2/Xe/Ce-TiO_2, O_3/Xe/Ce-TiO_2). In all cases, samples taken at different contact times up to 15 min were analyzed. An analytical method based on stir-bar sorptive extraction (SBSE), followed by comprehensive two-dimensional gas chromatography (SBSE-GC×GC-TOF-MS), was used for the automatic searching and evaluation of the synthetic musks and other nonpolar or semipolar contaminants in the wastewater samples. In all cases tonalide was more easily removed than galaxolide. The best results for the latter (more than 75% removal after 5 min on stream) were obtained from ozonation (O_3) and visible light photocatalytic ozonation (O_3/Xe/Ce-TiO_2). A significant removal of both pollutants (~60% after 15 min) was also obtained during visible light photocatalysis (O_2/Xe/Ce-TiO_2). UV radiation was able to deplete tonalide (+90%) after 15 min but only reduced the concentration of galaxolide to about half of its initial concentration. The toxicity of treated samples decreased for O_3/UV and O_3/Ce-TiO_2, but increased during irradiation processes UV, Xe and Xe/Ce-TiO_2. Ozone treatments tend to decrease toxicity up to a certain dosage, from which point the presence of toxic transformation products has adverse effects on aquatic microorganisms.

Keywords: Synthetic musks; Stir bar sorptive extraction (SBSE); Comprehensive two-dimensional gas chromatography (GC×GC); Ozonation; Ultraviolet irradiation; Visible light photocatalysis.

1. Introduction

Synthetic musks are currently manufactured and used in large amounts for incorporation in a wide variety of personal care products. Their role is to fix fragrances by slowing down the release of volatiles (Reiner and Kannan, 2006). Synthetic musks comprise a wide variety of substances, of which only nitro, polycyclic and macrocyclic derivatives have achieved any commercial importance. They are artificial substances which do not occur in the nature and do not share chemical or structural relationship with natural musks. Currently, nitro musks, a family comprising musk xylene and musk ketone, are being gradually displaced by polycyclic derivatives, which account for about three-quarters of the worldwide market (Sommer, 2004). Of these, 1,3,4,6,7,8-hexahydro-4,6,6,7,8,8-hexamethylcyclopenta(g)-2-benzopyran (HHCB, galaxolide®) and 7-acetyl-1,1,3,4,4,6-hexamethyltetrahydronaphthalene (AHTN, tonalide®) are by far the two largest volume products, representing about 95% of the EU market and 90% of the US market for all polycyclic musks (Clara et al., 2011).

The widespread use of synthetic musks leads to their release to the environment in large amounts through the discharge of wastewater treatment plants (WWTP). Rosal et al. (2010a) measured values of up to 25 μg/L of HHCB and 1.9 μg/L of AHTN in the influent of a wastewater treatment plant, very high figures compared with the 30 ng/L found for celestolide and 6 ng/L for traseolide. As a consequence, HHCB is one of the most abundant xenobiotic in untreated wastewater together with caffeine, its metabolite paraxanthine and the non-steroidal anti-inflammatory drug acetaminophen. According to their non-polar character, the removal efficiency of these compounds is high in conventional activated sludge WWTP, but their high concentration still leads to occurrences in the microgram per litre range in treated effluents (Bester, 2004; Ternes et al., 2007; Lv et al., 2010). In comparison, the average concentration of musk xylene and musk ketone have been found in the 50–100 ng/L range (Rosal et al., 2010a). Synthetic musks have also been detected in similar concentrations in environmental samples (Gómez et al., 2012). Bester

(2005) reported concentrations of up to 600 ng/L of polycyclic musks in the River Ruhr at the discharge point of a WWTP. In the part of the same river where drinking water is extracted, he found 60 ng/L HHCB and 10 ng/L AHTN. These are typical values for rivers in populated areas. In Korean surface waters Lee et al. (2010) reported concentrations in the 100–272 ng/L range for HHCB and 30-52 ng/L for AHTN. Synthetic musks are persistent compounds, a fact stressed by Schmid et al. (2007) who investigated their presence in lipid-based fish tissue from remote Alpine lakes. Although at levels far below those for fish from lakes and rivers receiving effluents of WWTP, HHCB and AHTN as well as other nitro and polycyclic musks were nonetheless still detectable on account of their entrance by atmospheric precipitation.

It has been shown that the biotransformation of HHCB into HHCB-lactone takes place in WWTP operating with activated sludge (Bester, 2004). The same author reported 20–30 ng/L HHCB-lactone in the River Ruhr at considerable distances from WWTP discharge points (Bester, 2005). HHCB-lactone was found in all samples taken from the River Henares (Madrid, Spain), with a profile along the river course similar to its parent compound HHCB. HHCB-lactone was found in the water samples at a comparable concentration or even higher than those for HHCB (Gómez et al. 2012). This metabolite has been identified in fish and water samples by other groups (Franke et al., 1999; Kallenborn et al., 2001). HHCB–lactone was found in all wastewater samples in the United States at concentrations in the 146-4000 ng/L range and in sludge at 3.16-22.0 mg/kg dry weight (Reiner et al., 2007). Besides its biological origin, some HHCB–lactone is included in the technical galaxolide product, so it can also be found at the plant entrance. While HHCB and AHTN concentrations decreased during treatment, the concentrations of HHCB-lactone increased in water after treatment from an average of 505 ng/L (897 ng/L) in the influent to 1620 ng/L (1740 ng/L) in the effluent of two WWTP receiving domestic (domestic and industrial) discharges in New York State (Reiner et al., 2007). Recently, Janzen et al. (2011) identified HHCB-lactone as transformation product from the ozonation of HHCB in pure water.

In spite of concern due to their persistence and potential to bioaccumulate, the toxicity and environmental risks of these chemicals have been usually regarded as low (Salvito, 2005). However, it has been demonstrated that nitro musks can behave as co-genotoxicants (Mersch-Sundermann et al., 2001) and musk xylene has been included in the Candidate List of Substances of Very High Concern of the European Chemicals Agency. Luckenbach and Epel (2005) showed that nitro and polycyclic musks can inhibit the activity of multidrug efflux transporters responsible for multixenobiotic resistance in the gills of a marine mussel (*Mytilus californianus*). Nitro musks were more effective inhibitors than polycyclic musks, with combined IC_{50} values of 0.82 ± 0.53 μM for nitro musks and 2.34 ± 0.82 μM for polycyclic musks. Moreover, a long term inhibition of efflux transporters results in the continued accumulation of normally excluded toxicants even after direct exposure to the musk has ended.

In this work, an analytical method based on stir-bar sorptive extraction (SBSE), followed by comprehensive two-dimensional gas chromatography (SBSE-GC×GC-TOF-MS) was used for the evaluation of synthetic musks (Balthussen et al., 1999). This technique has recently been proposed as a tool for the multiresidue analysis of priority and emerging contaminants in waters with excellent results in terms of separation efficiency, analysis time and detection limits (Prieto et al., 2007; Gómez et al., 2011). The depletion of HHCB and AHTN in biologically treated wastewaters spiked with environmentally relevant concentrations of both compounds was tracked. The treatments assayed were ozonation with and without the addition of hydrogen peroxide (O_3, O_3/H_2O_2), ultraviolet (254 nm low pressure mercury lamp) and xenon-arc visible light irradiation alone and in combination with ozone (UV, O_3/UV, Xe, O_3/Xe) and visible light photocatalytic oxidation using a cerium-doped titanium dioxide photocatalyst performed under continuous oxygen or ozone gas bubbling (O_2/Xe/Ce-TiO_2, O_3/Xe/Ce-TiO_2). In all cases, we analyzed samples taken at different contact times up to 15 min and monitored their toxicity for the microcrustacean *Daphnia magna*, the green alga *Pseudokirchneriella subcapitata* and the marine bacterium *Vibrio fischeri*.

2. Methodology

Materials

Galaxolide and tonalide were purchased from Dr. Ehrenstorfer (Augsburg, Germany). The reagents used for the analyses were analytical grade methanol and sodium chloride (> 99.5 %) supplied by J.T. Baker (Deventer, Holland) and analytical grade water from Fluka (Buchs, Switzerland). The solutions in pure water were prepared with water obtained from a Milipore Mili-Q system with a resistivity of at least 18 MΩ cm^{-1} at 25 ºC. The rest of the chemicals (purity > 95%) were purchased from Sigma-Aldrich. Wastewater samples were taken from the output of the secondary clarifier of a WWTP located in Alcalá de Henares (Madrid). The plant treats a mixture of domestic and industrial wastewater from facilities located near the city and has a nominal capacity of 3000 m^3/h of raw wastewater. Additional details are given elsewhere (Rosal et al., 2010a). Prior to the runs, wastewater aliquots were filtered using 0.45 μm glass fibre filters, analyzed and, for runs involving the use of ozone, pre-ozonated according to the procedure described below. For runs involving catalyst in suspension, treated samples were filtered prior to the analyses using the same 0.45 μm glass fibre filters. The main wastewater parameters are listed in Table 1. The samples were spiked before treatments with 500 ng/L of galaxolide or tonalide to ensure final concentrations below one microgram per liter, which represents the

lower range of concentration in treated wastewater (Rosal et al., 2010a).

Table 1. Wastewater characterization parameters for raw and pre-ozonated effluent

Parameters	raw wastewater	pre-ozonated effluent
pH	7.79 (in situ)	n.a.
TSS (mg/L)	20 (as received)	n.a.
Dissolved oxygen (mg/L)	8.7 (in situ)	n.a.
Conductivity (μS/cm)	875	802
Turbidity (NTU)	2.5	1.4
COD (mg/L)	28	20
NPOC (mg/L)	8.1	4.7
Hardness (mg/L $CaCO_3$)	219	221
N-NO_3 (mg/L)	9.8	10.5
N-NH_4 (mg/L)	0.8	0.7
SUVA 254 nm	1.7×10^{-2}	8.7×10^{-3}
Anions and cations		
Sulphate (mg/L)	79.9	80.1
Chloride (mg/L)	80.6	81.9
Phosphate (mg/L)	2.6	2.7
Sodium (mg/L)	70.5	70.2
Potassium (mg/L)	14.9	15.8
Magnesium (mg/L)	21.6	21.6
Calcium (mg/L)	52.2	53.0
Metals		
Chromium	13	
Cobalt	1.8	
Copper	1.7	
Lead	0.49	
Manganese	0.92	
Molybdenum	4.3	
Nickel	2.3	
Strontium	60	
Tin	0.29	
Titanium	0.93	
Vanadium	1.1	
Zinc	34	

n.a.: not analysed

The photocatalyst was a ceria-doped TiO_2 with 0.5% wt. of cerium prepared by sol–gel method. The synthesis was as follows. Solution A was prepared by adding 10 mL $Ti(O\text{-}Pr)_4$ to 50 mL ethanol. Solution B was prepared by dissolving 0.1842 g of $(NH_4)_2Ce(NO_3)_6$ in 10 mL ultrapure water and then immediately adding 40 mL ethanol and 10 mL glacial acetic acid under vigorous stirring. Solution A was then added dropwise to solution B, sonicated, dried at 100ºC and calcined in air at 670ºC for 1 h. The catalyst had a surface area (BET) of 29 m^2/g and average pore size (BJH, desorption) of 6.3 nm. The catalyst had a mean particle size of 547 ± 33 nm as determined by Dynamic Light Scattering and a ζ-potential of -49.6 ± 0.7 mV, which dropped to -16.7 ± 0.8 mV when dispersed in raw wastewater and to -14.0 ± 0.9 mV in pre-ozonated wastewater. The catalyst absorbed radiation from 290 nm (Pyrex cut-off). The band gap energy of the photocatalyst as obtained by UV/VIS spectroscopy was 2.63 eV (470 nm), 90 nm higher than anatase. The unit cell parameters of Ce-TiO_2 were calculated from X-ray diffraction (XRD) considering that TiO_2 anatase belongs to the tetragonal system, whose unit cell parameters comply with the equation $1/d_{hkl}^2 = (h^2+k^2)/a^2 + l^2/c^2$. The diffraction peaks from (1 0 1) and (0 0 4) planes were used, obtaining values of a = b = 3.78 Å and c = 9.49 Å, which essentially coincide with those for pure anatase.

Experimental setup and procedure

A scheme of the experimental setup for ozonation and irradiation is given in Fig. 1. Ozone was produced by a corona discharge and continuously bubbled throughout the run. Further details are given elsewhere (Rosal et al., 2008a). Irradiation experiments were performed using a 15W Heraeus Noblelight TNN 15/32 low-pressure mercury vapour lamp emitting at 254 nm and a Heraeus TQ Xe 150, Xe-arc lamp with spectral emission in the visible region. For visible light irradiation, an additional Pyrex tube acted as a filter absorbing wavelengths lower than 290 nm. The lamp sleeve was equipped with a quartz cooling tube in which the lamps were fitted and was refrigerated by means of a thermostatic bath. The temperature was kept at 25°C in all cases. Actinometric measurements allowed the fluence rates per unit volume to be determined: 6.01×10^{-6} E L^{-1} s^{-1} for the low-pressure mercury lamp and 1.05×10^{-6} E L^{-1} s^{-1} for the Xe-arc lamp. As chemical actinometers, hydrogen peroxide for the mercury lamp and 2-nitrobenzaldehide for the Xe-arc lamp, were used, the latter method basically recording the near UV part of the spectra in the 290-400 nm range (Nicole et al., 1990; Allen et al., 2000).

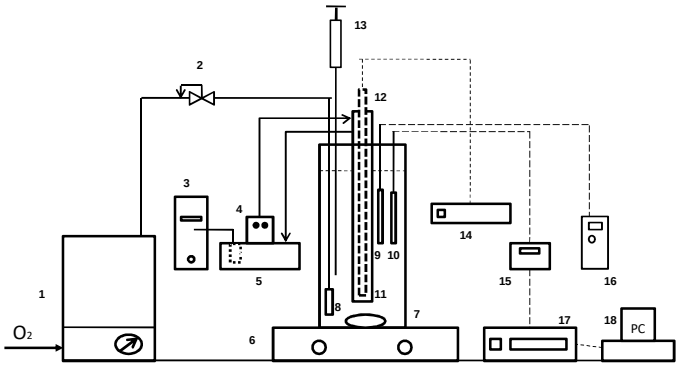

Figure 1. Experimental equipment: 1, ozone generator; 2, flow control; 3, cooling device; 4, thermostat; 5, bath; 6, magnetic stirrer; 7, reactor; 8, diffuser; 9, pH electrode; 10, ozone sensor; 11, cooling tube; 12, lamp; 13, sampling device; 14, power supply; 15, ozone analyser; 16, pH control unit; 17, data acquisition unit; 18, PC.

The experiments were carried out in batch mode in a vessel (1.3 L) agitated with a magnetic stirrer at 900 min^{-1}. Samples were taken for analysis at prescribed intervals. In ozonation runs the dissolved ozone was removed using

Table 2. Summary of experimental conditions used in this work.

No. and description		Process conditions
Processes involving homogeneous ozone		
1	O_3	Gas flow 0.19 N m^3 h^{-1} $C_{O_3(g)}$ 22 g Nm^{-3}
2	O_3/H_2O_2	H_2O_2 (30 %) 30 μL/L at 0 min and 7.5 min Ozone as in (1)
3	O_3/UV	15W Heraeus Noblelight TNN 15/32 mercury lamp Fluence rate 6.01 x 10^{-6} E L^{-1} s^{-1} (254 nm)
4	O_3/Xe	Heraeus TQ Xe 150, Xe-arc lamp Fluence rate 1.05 x 10^{-6} E L^{-1} s^{-1} (290-400 nm)
Catalytic and Photocatalytic processes		
5	O_3/Ce-TiO_2	200 mg/L catalyst agitated 30 min prior to the run Ozone as in (1)
6	O_3/Xe/Ce-TiO_2	Ozone as in (1) Irradiation as in (4) Catalyst as in (5)
7	Xe/Ce-TiO_2	Concentration of dissolved oxygen 31-33 mg/L kept throughout the treatment Irradiation as in (4) Catalyst as in (5)
8	Xe/Ce-TiO_2 (Raw wastewater)	Matrix: 0.45 μm filtered effluent Irradiation as in (4) Catalyst as in (5) Dissolved oxygen as in (7)
Photolytic processes without ozone		
9	UV	Irradiation as in (3)
10	UV (Raw wastewater)	Matrix: 0.45 μm filtered effluent Irradiation as in (3)
11	Xe	Irradiation as in (4)
12	Xe (Raw wastewater)	Matrix: 0.45 μm filtered effluent Irradiation as in (4)

sodium thiosulfate except for those samples used to measure the concentration of HHCB, AHTN and HHCB-lactone, in which ozone was stripped by bubbling nitrogen in order to avoid interferences with the analytical procedure. For all experiments pH was controlled at 7.5 within ± 0.1 units and close to the value measured in raw wastewater. The catalyst, when used, was loaded at a concentration of 200 mg/L and agitated 30 min prior to the runs in order to equilibrate surface charge. In ozonation runs, galaxolide and tonalide were dissolved in wastewater previously ozonated under the same conditions used for the runs until ozone appeared in solution. The reason for this procedure was to avoid interferences due to the presence of organic compounds which react rapidly with ozone (Rosal et al., 2010b). This would have kept ozone absent from the bulk and reaction would have taken place at the interface or in the liquid film. In these conditions, the exposure to hydroxyl radicals is not defined as it refers to the bulk (Buffle et al., 2006a). Besides, non-polar compounds tend to accumulate at the gas-liquid interface, so it was preferred to spike wastewater by the moment of appearing ozone in solution. Additional runs were performed in pure water using a 2 mM phosphate buffer at pH 7.5 prepared from 0.2 M $NaH_2PO_4 \cdot 2H_2O$ and 0.2 M Na_2HPO_4 solutions to avoid pH drift. Table 2 summarizes the experimental conditions used in this work.

Analyses

The analyses of water samples were carried out by stir-bar sorptive extraction (SBSE) followed by comprehensive two-dimensional gas chromatography (GC×GC-TOF-MS). Treated and untreated wastewater samples were extracted with 20 mm (length) x 0.5 mm (film thickness) PDMS commercial stir bars (Gerstel, Muelheim an der Ruhr, Germany). The coated stir bars were thermally desorbed using a thermal desorption unit (Gerstel) connected to a programmed temperature vaporization (PTV) system injector CIS-4 (Gerstel) by a heated transfer line at 300 °C. The PTV injector was installed in a GC×GC-TOF-MS system (Agilent 7890A gas chromatograph, equipped with an additional oven and a quad-jets modulator (two cold jets and two hot jets). Liquid nitrogen used for cooling was automatically filled from a 60 L Dewar liquid nitrogen storage tank. The first column was a 10 m x 0.18 mm i.d., 0.2 μm film thickness Rtx-5 coated with 5% diphenyl 95% dimethyl polysiloxane (Restek). The second column was a 1 m x 0.1 mm i.d., 0.10 μm film thickness Rxi-17 coated with 50% diphenyl 50% dimethylpolysiloxane (Restek). The MS system was a Pegasus 4D TOF (LECO Corporation). Details concerning the performance of the analytical method as well as sample preparation can be found elsewhere (Gómez et al., 2011). A hybrid triple quadrupole/Linear Ion Trap mass spectrometer system (5500 QTRAP® LC/MS/MS, AB Sciex Instruments, Foster City, CA) coupled to an HPLC, Agilent 1200 (Agilent Technologies, Wilmington, DE, USA) with an electrospray interface was used for the structural elucidation of HHBC-lactone using ozonated or irradiated mixtures of HHBC diluted in pure water. The analytical column employed was a reversed-phase C8 of 150 mm × 4.6 mm and 5 μm particle size (Agilent ZorbaxEclipse XDB). Details on the analytical procedure have been given elsewhere (Martínez-Bueno et al., 2011). The analyses of p-chlorobenzoic acid (pCBA) were performed by HPLC using an Agilent 1200 apparatus equipped with a reversed phase Kromasil 5u 100A C18 analytical column. The mobile phase (flow rate 1mL/min) was a 40:60 mixture of water containing 4mL/L of orthophosphoric acid and 50 mL/L of methanol and acetonitrile. UV detection was carried out at 280 nm.

Non Purgeable Organic Carbon (NPOC) was determined by means of a Shimadzu TOC-VCSH total carbon organic analyzer. Anions were determined using a Metrohm 861 Advance Compact IC with suppressed

conductivity detector and a Metrosep A Supp 7-250 analytical column with 36 mM Na_2CO_3 as eluent with a flow of 0.8 mL min^{-1}. Cations were quantified by means of a Metrosep C3 column using 5.0 mM HNO_3 as eluent with a flow of 1 mL min^{-1}. The content of trace metals in the wastewater was assessed by Inductively Coupled Plasma-Mass Spectrometry using a quadrupole mass spectrometer Agilent 7700X operating at 3 MHz in helium cell gas mode. The concentration of ozone dissolved in the aqueous phase was monitored with an amperometric Mettler Toledo 358/210 dissolved ozone sensor calibrated using the Indigo Colorimetric Method (SM 4500-O3 B). The signal was transmitted to a Mettler Toledo Thornton M300 and finally monitored and recorded using an Agilent 34970 Data Acquisition Unit connected to a computer. The concentration of ozone in gas phase was determined using an Anseros Ozomat GM6000 Pro photometer calibrated against potassium iodide.

The catalyst was characterized by *x-ray diffraction* (*XRD*) using a *Seifert 3000P diffractometer* (Cu Kα, λ = 1.5406 Å). The BET specific surface was determined by nitrogen adsorption at 77 K using a SA 3100 Beckman Coulter Analyzer. The size distribution of catalyst particles (< 5000 nm) was obtained using dynamic light scattering (DLS, Malvern Zetasizer Nano ZS). Zeta potential was measured via electrophoretic light scattering combined with phase analysis light scattering in the same instrument. The measurements were conducted at 25ºC using 2 mM phosphate buffer at pH 7.5 as the dispersing medium. The absorbance of the photocatalyst was measured using a UV/VIS/NIR Perkin Elmer Lambda 900 spectrometer equipped with integrating sphere.

Toxicity assessment

The toxicities of raw, spiked and treated wastewater samples were assessed using the following bioassays: multigenerational growth inhibition of the green alga *Pseudokirchneriella subcapitata*, the inhibition of the constitutive luminescence of the marina bacterium *Vibrio fischeri*, and the immobilization of the microcrustacean *Daphnia magna*. This amounts to the combination of acute and multigenerational assays and the combined use of prokaryotic and eukaryotic organisms at two trophic levels. Phenol, $ZnSO_4$ and $K_2Cr_2O_7$ have been used as toxicity standards and all tests have been replicated to ensure reproducibility and in order to obtain acceptable confidence intervals.

The algal growth inhibition test followed the procedure described in OECD TG 201 *P. subcapitata* open system (OECD, 2011). Prior to the test hydrogen peroxide was removed using 5 µL of catalase solution 5000 mg/L (3691 U/mg bovine liver obtained from Sigma-Aldrich) per 1 mL of sample. This procedure removed excess H_2O_2 in O_3/H_2O_2 and the H_2O_2 that could have been produced as secondary oxidant in other processes. The cultures used the OECD growth medium at pH adjusted to 8.0 ± 0.1 Algal cells were first cultured in 25 mL agitated flasks. The prescribed number of cells was transferred to 96-well clear disposable microplates and exposed to pollutants during the logarithmic growth phase. The total volume occupied was 220 µL, each well containing 180 µL of sample, 20 µL of a concentrated OECD growth medium and 10 µl of microalgae. The microplates were placed in an algal growth chamber under continuous fluorescent illumination (approximately 100 µE m^2 s^{-1}), and incubated at 22 ± 1 °C. The growth of *P. subcapitata* was monitored daily for 72 h and assessed by chlorophyll fluorescence (Excitation 444 nm – Emission 680 nm) using a Fluoroskan Ascent FL plate fluorometer-luminometer.

Bioassays with the photo luminescent bacteria *V. fischeri* were carried out according to ISO 11348-3 standard protocol (International Organization for Standardization, 2007). This bioassay measures the decrease in bioluminescence due to the presence of a toxic substance. The commercial Biofix Lumi test (Macherey-Nagel, Germany) was used. The measurements were performed at 16.5 ± 0.8°C using a Fluoroskan Ascent FL plate luminometer. The effect of toxics was measured as percentage of inhibition with respect to the light emitted in the absence of any toxic influence after 30 min exposure. In treated wastewater, the reference was always the same wastewater after adjusting osmotic pressure.

Acute immobilization tests with *D. magna* were conducted following the standard protocol described in the European Guideline OECD TG 202 (OECD, 2004). The *D. magna* bioassay used a commercially available text kit (Daphtoxkit F™ magna, Creasel, Belgium). The dormant eggs were incubated in standard culture medium imitating natural fresh water at 20 ± 1°C under continuous illumination of 6000 lx in order to induce hatching. Between hatching and test steps, the daphnids were fed with the microalga Spirulina to avoid mortality during tests. Neonates were incubated for 48 h in the dark at 20°C, the pH of samples being adjusted to the tolerance interval of this organism (Seco et al. 2003). Acute toxicity was assessed by observing the mobility of *D. magna*: the neonates were considered immobilized if they lay on the bottom of the test plate and did not resume swimming within 15 s.

3. Results and discussion

Efficiency of hydroxyl radical formation during ozonation and irradiation processes

The removal of dissolved organics by ozone is due to the combination of direct and indirect reactions, the latter essentially being reactions with hydroxyl radicals. Elovitz and von Gunten (1999) proposed a parameter R_{ct} to characterize the ozonation process by measuring the exposure to hydroxyl radicals. They defined a ratio between integral ct-exposures to hydroxyl radicals and ozone as follows:

$$R_{ct} = \frac{\int_o^t c_{HO^\bullet}.\, dt}{\int_o^t c_{O_3}\, dt} \qquad [1]$$

The parameter can be readily obtained using a p-chlorobenzoic acid (pCBA) as probe compound since its direct ozonation rate constant is negligible. The R_{ct} parameter depends on matrix composition and can be applied to evaluate the efficiency of ozonation and ozone-based disinfection processes in natural waters (Elovitz and von Gunten, 1999). Its suitability for wastewaters has been shown in previous works (Rosal et al., 2008b & 2010a). It has also been determined that hydroxyl radical exposure may be very high during the initial phase of ozonation runs. In fact, before ozone appears in solution during the fast kinetic regime, there is a significant exposure which cannot be measured using Eq. 1. The initial phase also contributes to a high proportion of the ozone consumption but, as a consequence of the low concentration of dissolved ozone, it accounts for a small or negligible proportion of the overall ozone-exposure. R_{ct} decays thereafter and attains a steady state once the slow kinetic regime has been achieved (Buffle et al., 2006b). This two-period pattern is particularly clear in waters with low concentration of radical scavengers for which R_{ct} can be several orders of magnitude higher during the first ozonation period.

In this work, R_{ct} was measured before and after the second minute on stream, which was the time necessary to ensure slow kinetic regime in all ozonation runs (Rosal et al., 2010a). The corresponding data are given in the lower part of Fig. 2 for O_3 and O_3/H_2O_2 homogeneous systems; for catalytic, O_3/Ce-TiO_2, and photocatalytic, O_3/Xe/Ce-TiO_2 ozonation and for the photolytic treatments O_3/Xe and O_3/UV. The results depicted in Fig 2 were obtained by spiking wastewater with up to 1 mg/L of pCBA in phosphate buffered pure water, identified as "pure water", and in pre-ozonated wastewater prepared as described above. In pure water runs, the rapid decay of pCBA meant sufficient data could not be obtained in order to evaluate R_{ct} under slow kinetic regime. Generally, R_{ct} values were much lower in wastewater than in pure water due to the presence of bicarbonates and other radical scavengers. As expected, O_3/H_2O_2 and O_3/UV resulted in higher values of R_{ct} as both H_2O_2 and UV accelerate the decomposition of ozone and provide an additional source of hydroxyl radicals. The combined use of ozone and radiation (O_3/UV) led to the highest R_{ct} values, in both pure water and in wastewater, whereas for the rest the values observed were in the 10^{-7}-10^{-8} range and exhibited the typical two-phase pattern described before. The combined use of ozone and visible radiation (O_3/Xe) including photocatalysis (O_3/Xe/Ce-TiO_2) did not result in any significant reduction of R_{ct} in wastewater samples, although the effect of Ce-TiO_2 was apparent in pure water, with R_{ct} for O_3/Xe/Ce-TiO_2 one order of magnitude higher for non-catalytic O_3/Xe and catalytic O_3/Ce-TiO_2 ozonation. Most probably, the presence of oxidizable compounds and radical scavengers reduced the production of the hydroxyl radicals detected by pCBA.

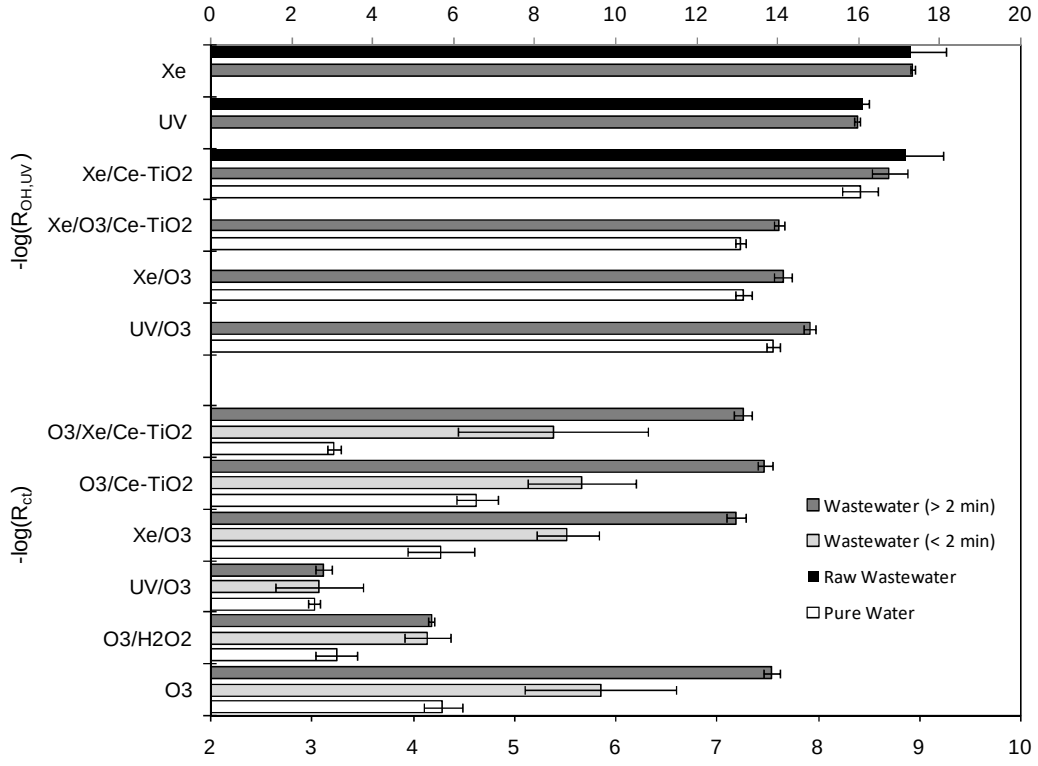

Figure 2. Radical exposure parameters R_{ct} and $R_{OH,UV}$ for ozone and radiation-based processes in pure water and wastewater. (Note that higher values of $-log(R_{ct})$ or $-log(R_{OH,UV})$ represent lower generation of hydroxyl radicals.)

The presence of HHCB and AHTN in spiked treated wastewater does not introduce any significant change in the slow/rapid kinetic regime pattern. These compounds were added in very small concentrations and their rate constant for the direct ozonation reaction were not high. Nöthe et al. (2007) determined rate constants for the reaction of HHCB and AHTN with molecular ozone of 8 $M^{-1}\,s^{-1}$ and 140 $M^{-1}s^{-1}$, respectively. The removal of both compounds due to stripping was not significant for the experimental conditions used in this work.

The radical exposure per fluence ratio due to irradiation, $R_{OH,UV}$, was determined according to the method proposed by Rosenfeldt et al. (2006):

$$R_{OH,UV} = \frac{\int_o^t c_{HO^\bullet}\, dt}{E_o^{'}\, t} \qquad [2]$$

where $R_{OH,UV}$ is the hydroxyl radical exposure per UV fluence expressed in (M L mW^{-1}) and $E_o^{'}$ the average UV fluence rate per unit volume (mW L^{-1}). pCBA was used as probe compound to determine the exposure to hydroxyl radicals as indicated elsewhere (Santiago et al., 2011). As shown in Fig. 2, $R_{OH,UV}$ was higher for photocatalytic and photolytic ozonation as a consequence of the dual mechanism of hydroxyl radical generation. The low, but quantifiable values obtained for $R_{OH,UV}$ under UV-filtered Xe irradiation were probably the result of the photolysis of nitrate (and nitrite), which is known to result in the formation of hydroxyl radicals (Mack and Bolton, 1999). Otherwise, no measurable formation of hydroxyl radicals should be expected. In pure photolytic and photocatalytic processes Xe, UV and Xe/Ce-TiO_2, $R_{OH,UV}$ were almost constant throughout the runs in the 10^{-16} order; i.e., they did not exhibited the two-phase pattern observed in ozonation. The combined use of ozone and radiation reduced $R_{OH,UV}$ by about three orders of magnitude.

Removal of galaxolide and tonalide

In the wastewater samples used in this work, the concentrations of HHCB and AHTN were 1849 ng/L and 438 ng/L, respectively, dropping after pre-ozonation to 590 ng/L (HHCB) and 98 ng/L (AHTN). This represented a removal of ~ 70% for both compounds during the fast ozonation period before the ozone in solution was recorded. Fig. 3 (a and b) shows the variation in the relative concentrations of HHCB and AHTN in spiked wastewater throughout the treatments assayed in this work. For the sake of clarity, experimental errors are indicated as bars only in the case of xenon irradiation runs since this treatment did not result in any significant degradation of HHCB or AHTN. Error bars were calculated from the initial concentrations of HHCB and AHTN in samples directly taken from the reactor in the nine treatments assayed and therefore represent the variability associated with sample preparation and the analytical procedure. In all cases AHTN was more easily removed than HHCB, with a final concentration below 100 ng/L (representing > 90% removal efficiency) for O_3, O_3/UV, O_3/H_2O_2, O_3/Xe and for UV irradiation alone. The best removal efficiencies were obtained for HHCB in O_3, O_3/Xe and O_3/Xe/Ce-TiO_2, while UV-based processes, particularly UV photolysis gave poorer results with depletion close to 50% after 15 min of irradiation. It is interesting to note that catalytic ozonation did not result in better removal efficiencies for either compound, probably because of the low affinity of the catalyst surface with these non-polar compounds. The absence of adsorption of HHCB and AHTN was assessed by performing adsorption experiments under non-oxidizing conditions and analyzing samples taken after the same period used for reactions. Xe/Ce-TiO_2 photocatalysis resulted in depletion of 71 % and 83% for HHCB and AHTN, respectively, in 15 min on stream, which was close to the values for ozone and UV irradiation-based treatments, which were considerably more efficient at generating hydroxyl radicals.

Fig. 3c also shows the evolution of HHCB-lactone, the concentration of which was 250 ng/L in the spiked pre-ozonated wastewater (103 ng/L in RWW). In most runs, but particularly for O_3/UV and O_3/Xe the concentration of HHCB-lactone increased during the first minutes on stream. This proved that HHCB-lactone was formed as an intermediate transformation product during the ozone treatment of effluents containing HHCB, but also during UV irradiation as observed in Fig. 4. O_3, O_3/UV and O_3/H_2O_2 reduced HHCB-lactone concentrations by up to 25% of its initial value after 15 min.

Fig 4a displays the GC×GC contour plot with all the main compounds detected in the wastewater effluent represented as dots in a bidimensional plot in which the first (x-axis) and second (y-axis) dimensions represent retention times in a non-polar (Rtx-5) column and a polar (Rxi-17) column respectively. In this particular case, the signal-to-noise ratio was set to 10. For this application, in which several thousand compounds could be present in similar concentrations in the mixture, the choice of the second column was particularly critical as noted and discussed elsewhere (Gómez et al., 2011). The two-dimensional chromatogram allows both targeted and non-targeted compounds to be separated and identified. Fig. 4a also shows the mass spectra identification of HHCB, AHTN and HHBC-lactone, which in fact represent two isomers (cis- and trans- each with two enantiomers that could be resolved with the GC×GC technique at high dilution rates) with slightly different retention times, but perfectly separated in the bidimensional chromatogram. It can be observed that the deconvoluted mass spectra of the compounds in the acquired sample match the reference library spectra perfectly with a similarity score above 900. It is important to note that the resolution reached with the GC×GC technique allows most compounds to be separated from matrix components, a feature which is essential for their further identification in TOF–MS. The identification of HHCB-lactone was based on accurate mass measurements recorded by the

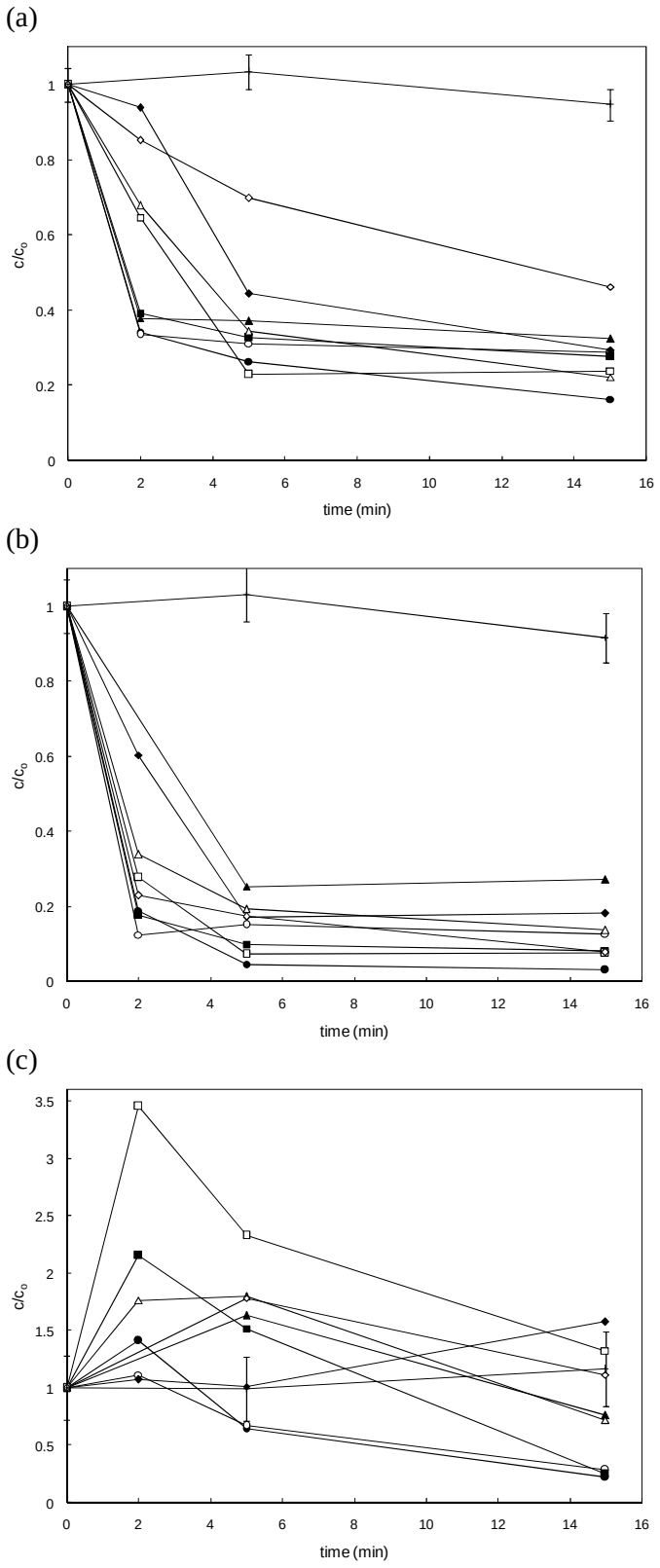

Figure 3. Concentration profiles for HHCB (a), AHTN (b) and HHCB-lactone (c) during the different treatments assayed: O_3 (●), O_3/H_2O_2 (○), O_3/UV (■), O_3/Xe (□), O_3/Ce-TiO_2 (▲), O_3/Xe/Ce-TiO_2 (Δ), Xe/Ce-TiO_2 (♦), UV (◊), Xe (+)

LC-TOF-MS instrument described above operating in positive mode (ESI+). These measurements allowed elemental composition to be proposed for the protonated $[M+H]^+$ *molecular* ions and their characteristic ion fragments, so providing a high degree of confidence in structure assignation. The accurate mass measurements recorded for the protonated HHCB-lactone (*m/z* 273.1850 for $C_{18}H_{25}O_2$) offer an excellent agreement of 0.2 ppm error with calculated *m/z* value. The main fragments (at *m/z* 255.1743, 225.1274 and 197.1325) correspond to the breaking of the benzopyrone moiety of HHCB-lactone with errors < 0.1, 4.8 and 6.5 ppm respectively.

The sequence of chromatograms represented in Fig. 4b displays the evolution of the target compounds HHCB, AHTN and HHBC-lactone during O_3/H_2O_2. In order to visualize peak intensity in the two-dimensional image, a bubble-type plot was used in which the bubble radius is proportional to the relative area of the peak represented. It is relative because for each sample the maximum radius size is proportional to the most concentrated compound in it. The absence of background in Fig. 4b is due to the filtering of the mass-spectra in order to display target compounds only.

Toxicity of raw and treated samples

Under the conditions of moderate TOC removal encountered in practical forms of AOP, the formation of transformation products with enhanced toxicity for aquatic organisms seems to be the rule rather than the exception (Rosal et al., 2009; Gómez-Ramos et al., 2011). Accordingly, in the runs reported in this work, organic carbon removal was not high. Measured as NPOC, it ranged from 2-15% after 15 min on stream except for O_3/H_2O_2 for which it reached ~40% in accordance with the oxidizing capacity of this system. Xe irradiation was also an exception, as no significant mineralization took place. The evolution of the toxicity of treated wastewater to *P. subcapitata* is shown in Fig. 5. The dotted line represents the growth rate of the green alga under control conditions. Values above 1 represent non-toxic mixtures or toxicity reduction, whereas lower values indicate growth inhibition. During Xe and UV (Hg lamp) irradiation and Xe/$CeTiO_2$ photocatalysis, the toxicity of the reaction mixture increased during the treatment, attaining in the case of UV a value as low as 60% of algal growth (UV 15 min, with respect to spiked pre-ozonated wastewater before irradiation). This reflects the formation and accumulation of toxic transformation products. Conversely, ozonation runs, and particularly O_3/UV led to higher algal growth and therefore a reduction in the toxicity of the reaction mixture. It is interesting to note that catalytic ozonation, $O_3/CeTiO_2$, a non-photolytic process with modest hydroxyl radical generation, led to mixtures in which toxicity always decreased over treatment time. For more intense processes such as O_3/H_2O_2 or homogeneous ozonation, the toxicity of the mixtures treated during 15 min was higher than that of non-treated spiked wastewater. In O_3/H_2O_2, in particular, the toxicity increased in all samples except the first, taken after 2 min. In photolytic ozonation, O_3/Xe, O_3/Xe/$CeTiO_2$ and O_3/UV a higher toxicity was observed in samples treated for longer periods. This indicates that efforts to reduce dissolved carbon concentrations are not necessarily followed by a fall in toxicity in treated effluents. On the contrary, the effect may be an increase in the concentration of toxic

(a)

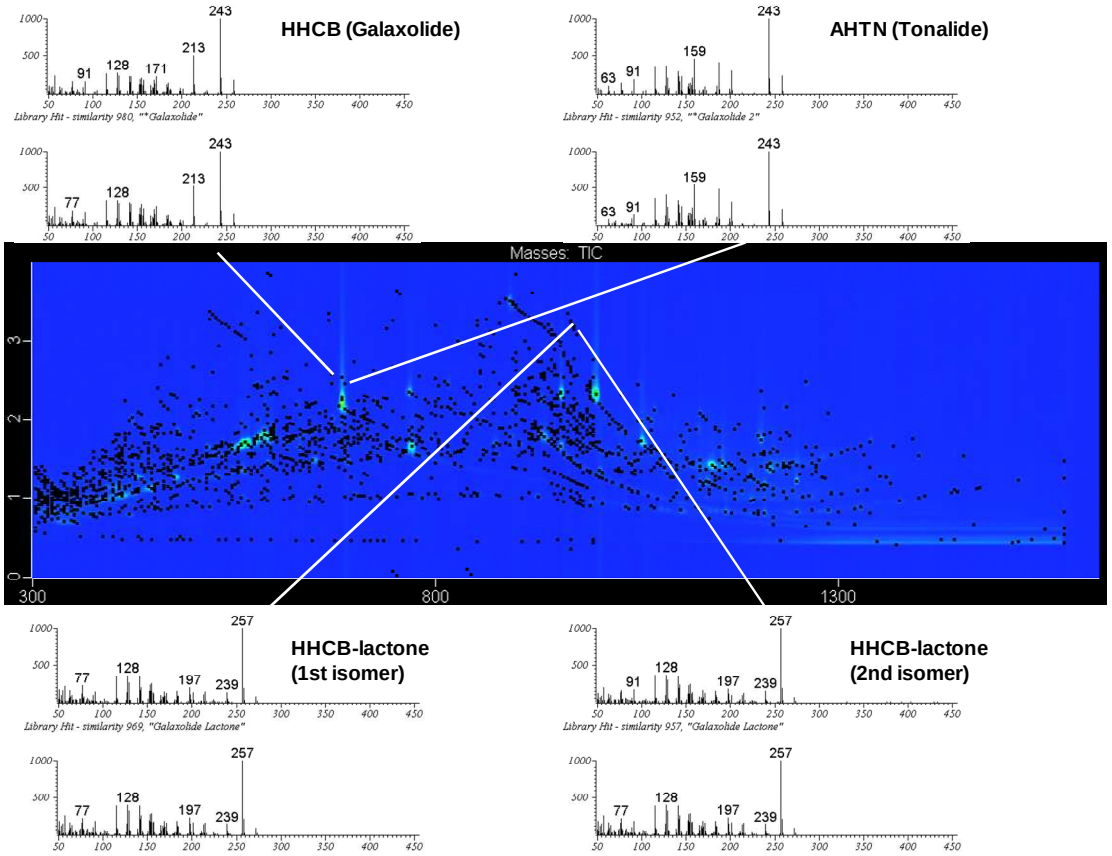

(b)

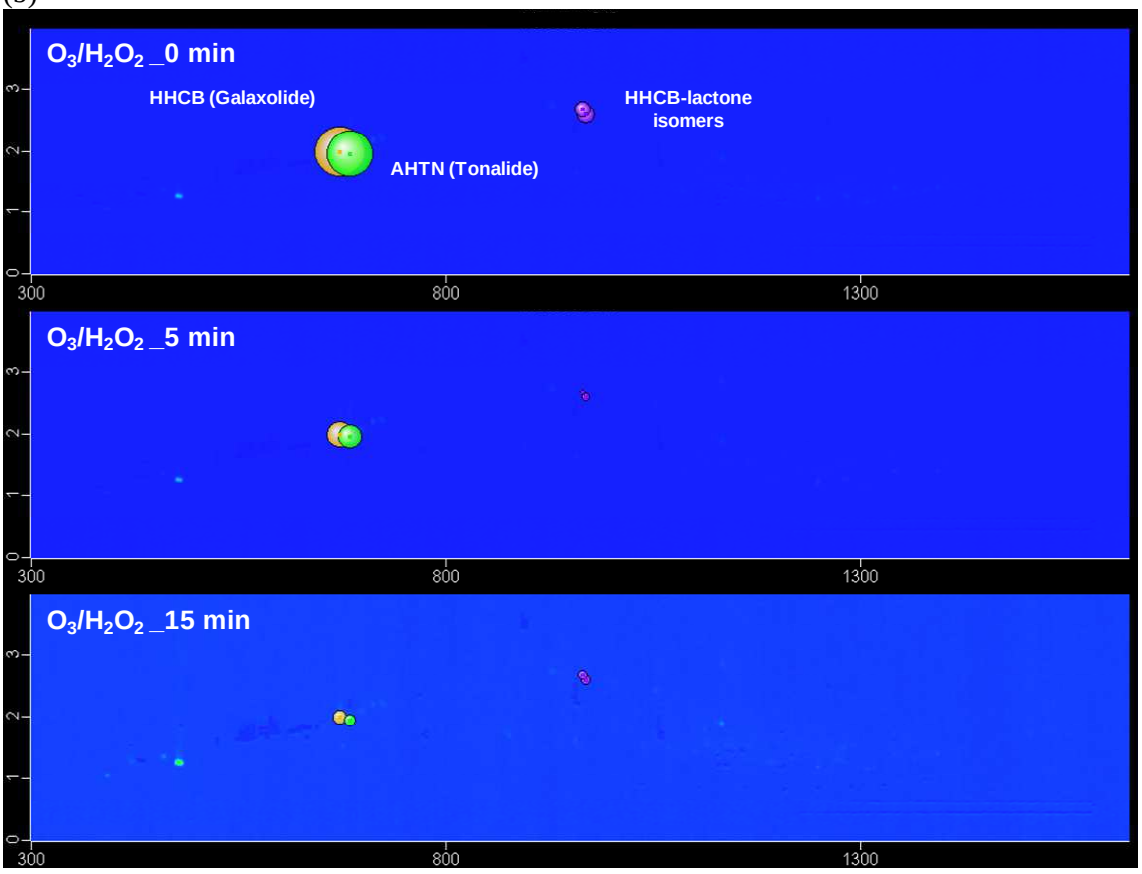

Figure 4. (a) GC×GC-TOFMS contour plot of spiked wastewater before treatment, showing the peaks and the spectra library searches for HHCB, AHTN and HHCB-lactone. (b) GC×GC-TOFMS bubble plot showing temporal variation of target compounds.

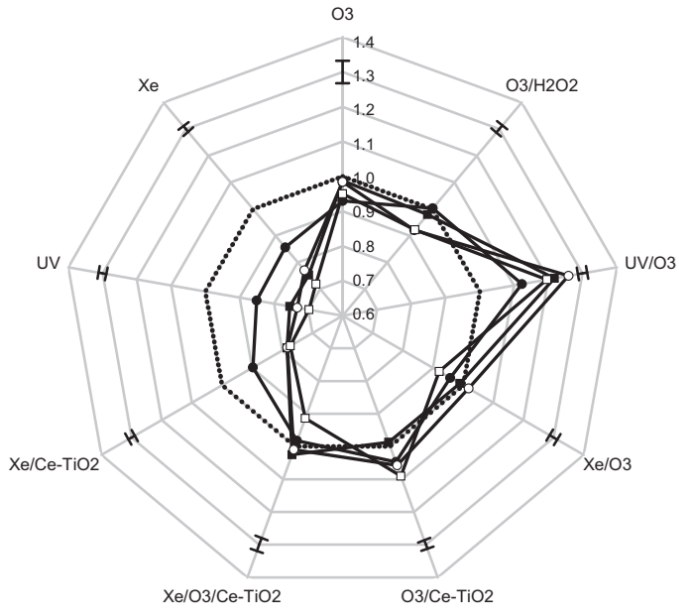

Figure 5. Toxicity of treated samples: relative growth rate of *P. subcapitata* (higher values correspond to lower toxicity; 1 = control). Time on stream: (●) 2 min, (■) 5 min, (○) 10 min, (□) 15 min. Dotted line: untreated pre-ozonated wastewater. (The bars represent confidence intervals.)

compounds. After 5 min, the concentration of the target compounds HHBC and AHTN did not suffer significant reductions, while the toxicity of samples treated for an additional 10 min period generally increased. Whenever significant changes in toxicity were encountered, most of the variations in the algal growth rate took place during the first 2 min on stream. These facts indicated that prolonged irradiation or ozonation treatments bring no benefits in terms of HHBC/AHTN removal or toxicity reduction.

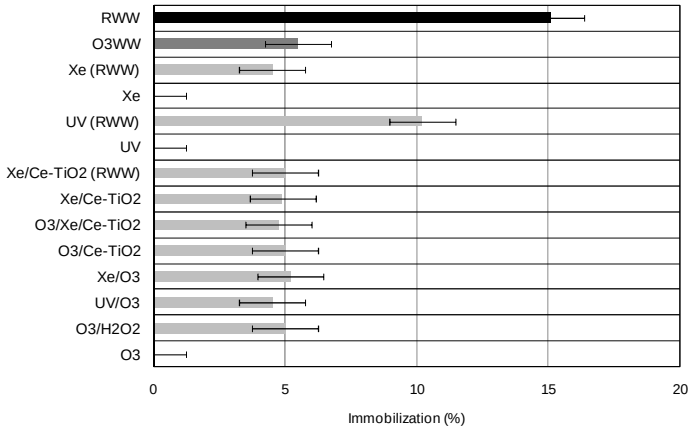

Figure 6. Toxicity assessed by immobilization of *D. magna*. RWW: Raw wastewater, O3WW: pre-ozonated wastewater before treatment.

Raw filtered wastewater was relatively toxic to *D. magna*, with an immobilization percentage of 15% for a contact time of 48 h. The toxicity of ozonated wastewater dropped to ~5%, the toxicity level observed after most treatments (Fig. 6). Only ozonation and UV or Xe irradiation of pre-ozonated wastewater led to lower immobilization, but the differences were not high, remaining close to the experimental error. It is interesting to note that the UV irradiation of raw, non pre-ozonated wastewater reduced toxicity by 5% up to a 10% immobilization, an effect that can only be attributed to the photolysis of toxic compounds in wastewater: the effect of UV on the other two species tested in this work, was the opposite.

A greater effect was observed using the marine bacteria *V. fischeri*, whose constitutive luminescence decayed considerably during UV, Xe and Xe/Ce-TiO_2 treatments. This is represented in Fig. 7 as relative bioluminescence, with lower values corresponding to more intense toxic effect. The lowest toxicities were observed for O_3/UV, O_3/Xe and O_3/Ce-TiO_2 treatments, in good agreement with the results obtained for *P. subcapitata*. Again, for O_3/H_2O_2, O_3 a decrease in toxicity was followed by an upturn at 2 min processing time. Once more, further treatment would be justified neither to remove micropollutants nor for its effect on the toxicity of treated effluent.

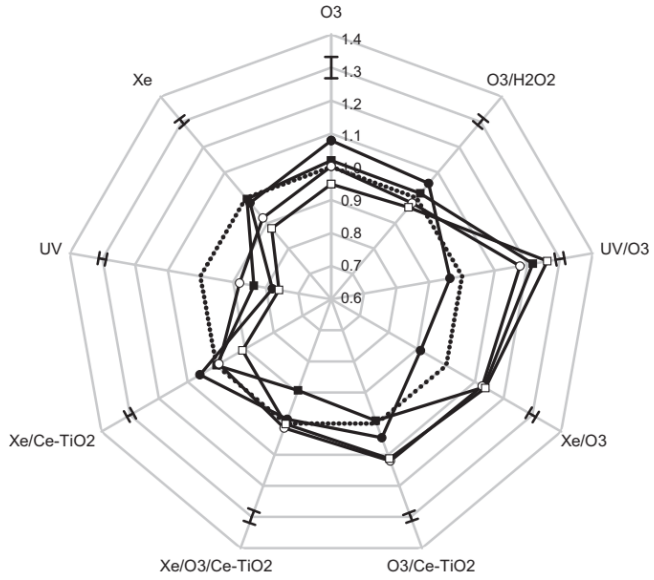

Figure 7. Toxicity of treated samples: relative luminescence of *V. fischeri* (higher values correspond to lower toxicities; 1 = control). Time on stream: (●) 2 min, (■) 5 min, (○) 10 min, (□) 15 min. Dotted line: untreated pre-ozonated wastewater. (The bars represent confidence intervals.)

The background toxicity of wastewater decreased with pre-ozonation both for *P. subcapitata* and *V. fischeri*. The relative (to pre-ozonated wastewater) growth inhibition of raw wastewater for *P. subcapitata* was 0.76 ± 0.04, whereas the bioluminescence inhibition of *V. fischeri* was 1.32 ± 0.10, which represented a 25-30% toxicity reduction in both cases. This effect must be due to the reaction of ozone with compounds with high direct ozonation rate constants, as it took place before ozone appeared in solution. Contrary to the generation of toxic transformation products observed with treatments like UV or high contact time ozonation, a low ozone dosage allowed the target pollutant to be removed without

producing compounds which were toxic for microorganisms.

A significant part of wastewater toxicity could be attributed to dissolved toxic metals, particularly zinc, mercury and other heavy metals. In this case, the amount of dissolved zinc in raw wastewater (34 μg/L) was close to the median effect value (EC_{50}) of 60 μg/L in *P. subcapitata* reported by Franklin et al. (2007). On the other hand, *D. magna* and *V. fischeri* are relatively insensitive to zinc as their EC_{50} lie in the mg/L range (Vesela et al., 2007; Ytreberg et al., 2010). In fact, ozone may lead to the separation of dissolved metals in the form of insoluble oxides. The parallel effect obtained for *V. fischeri* and *P. subcapitata* using pre-ozonated wastewater under different treatments, suggests that its toxicity was associated to the presence of organic pollutants that were eventually able to be removed by oxidation processes.

4. Conclusions

The combined use of ozone and radiation (O_3/UV) or hydrogen peroxide (O_3/H_2O_2) increased R_{ct} by three orders of magnitude. Ozone-radiation combined treatments also increased $R_{OH,UV}$ due to the effect of a dual source of hydroxyl radicals.

AHTN was more easily removed than HHCB, with best removal efficiencies for O_3, O_3/UV, O_3/H_2O_2, O_3/Xe and for UV irradiation alone. The depletion of HHCB was higher in ozone-driven treatments, while UV-based processes, particularly UV photolysis gave poorer results. Xe/Ce-TiO_2 photocatalysis, whose efficiency in generating hydroxyl radicals was relatively low, led to AHTN and HHCB degradation close to those obtained during ozonation treatments.

The concentration of HHCB-lactone increased during ozonation treatments at least during the first minutes, thus proving that HHCB-lactone is formed as an intermediate transformation product from HHCB. For this reason, most ozone treatments only resulted in moderate reductions in HHCB-lactone concentration. In the best case the depletion of initial HHCB-lactone reached about 75% for O_3, O_3/UV and O_3/H_2O_2.

Radiative treatments, particularly germicidal UV, but also Xe/$CeTiO_2$ photocatalysis, led to an increase in toxicity for *P. subcapitata* and *V. fischeri*. This was most probably a consequence of the formation and accumulation of toxic transformation products from the oxidation of wastewater components.

Ozonation treatments, including O_3/UV but also catalytic ozonation O_3/Ce-TiO_2, O_3/Xe and O_3/Xe/Ce-TiO_2 resulted in initial toxicity reduction for short contact times, but the toxicity of treated wastewater to *P. subcapitata* and *V. fischeri* increased thereafter.

The results showed that prolonged irradiation or ozonation treatments offer no advantages in terms of HHBC/AHTN removal or toxicity reduction.

Acknowledgements

This work has been financed by the Dirección General de Universidades e Investigación de la Comunidad de Madrid, Research Network 0505/AMB-0395. The authors are also grateful to the Spanish Ministry of Science and Innovation (Project CTM2011-27657) for its economic support. One of the authors, JSM, would like to thank the Spanish Ministry of Education for the award of a FPU grant.

References

Allen, J.M., Allen, S.K., Baertschi, S.W., 2-Nitrobenzaldehyde: a convenient UV-A and UV-B chemical actinometer for drug photostability testing. J. Pharm. Biomed. Anal. 24, 167–178, 2000.

Baltussen, E., Sandra, P., David, F., Cramers, C.A., Stir bar sorptive extraction (SBSE), a novel extraction technique for aqueous samples: theory and principles. J. Microcol. Sep. 11, 737-747, 1999.

Bester, K., Polycyclic musks in the Ruhr catchment area—transport, discharges of waste water, and transformations of HHCB, AHTN and HHCB-lactone. J. Environ. Monit. 7, 43–51, 2005.

Bester, K., Retention characteristics and balance assessment for two polycyclic musk fragrances (HHCB and AHTN) in a typical German sewage treatment plant. Chemosphere 57, 863–870, 2004.

Buffle, M.O., Schumacher, J., Meylan, S., Jekel, M., von Gunten, U., Ozonation and advanced oxidation of wastewater: effect of O_3 Dose, pH, DOM and HO•-scavengers on ozone decomposition and HO• generation. Ozone Sci. Eng. 28, 247–259, 2006a.

Buffle, M.O., Schumacher, J., Salhi, E., Jekel, M., von Gunten, U., Measurement of the initial phase of ozone decomposition in water and wastewater by means of a continuous quench-flow system: application to disinfection and pharmaceutical oxidation, Water Res. 40, 1884–1894, 2006b.

Clara, M., Gans, O., Windhofer, G., Krenn, U., Hartl, W., Braun, K., Scharf, S., Scheffknecht, C., Occurrence of polycyclic musks in wastewater and receiving water bodies and fate during wastewater treatment. Chemsphere 82, 1116–1123, 2011.

Elovitz, M.S., von Gunten, U., Hydroxyl radical/ozone ratios during ozonation processes I. The R_{ct} concept, Ozone Sci. Eng. 21, 239–260. 1999.

Franke, S., Meyer, C., Heinzel, N., Gatermann, R., Hühnerfuss, H., Rimkus, G., Konig, W.A., Francke, W., Enantiomeric composition of the polycyclic musks HHCB and AHTN in different aquatic species. Chirality 11, 795–801, 1999.

Franklin, N. M., Rogers, N. J., Apte, S. C., Batley, G. E., Gadd, G. E., Casey, P. S. Comparative toxicity of nanoparticulate ZnO, bulk ZnO, and ZnCl2 to a freshwater microalga (*Pseudokirchneriella subcapitata*): the importance of particle solubility. Environ. Sci. Technol. 41, 8484–8490, 2007.

Gómez, M.J., Herrera, S., Solé, D., García-Calvo, E., Fernández-Alba, A., Automatic searching and evaluation of priority and emerging contaminants in wastewater and river water by stir bar sorptive extraction followed by comprehensive two-dimensional gas chromatography-time-of-flight mass spectrometry. Anal. Chem. 83, 2638–2647, 2011.

Gómez, M.J., Herrera, S., Solé, D., García-Calvo, E., Fernández-Alba, A.R., Spatio-temporal evaluation of organic contaminants and their transformation products along a river basin affected by urban, agricultural and industrial pollution. Sci. Total Environ. in press, DOI: 10.1016/j.scitotenv.2012.01.029

Gómez-Ramos, M.M., Mezcua, M., Agüera, A., Fernández-Alba, A.R., Gonzalo, S., Rodríguez, A., Rosal, R., Chemical and toxicological evolution of the antibiotic sulfamethoxazole under ozone treatment in water solution, J. Hazard. Mater. 192, 18–25, 2011.

International Organization for Standardization. Water Quality-Determination of the Inhibitory Effect of Water Samples on the Light Emission of *Vibrio fischeri* (Luminescent Bacteria Test). ISO 11348-3 revised version, Geneva, Switzerland, 2007.

Janzen, N., Dopp, E., Hesse, J., Richards, J., Türk, J., Bester, K., Transformation products and reaction kinetics of fragrances in advanced wastewater treatment with ozone, Chemosphere 85, 1481–1486, 2011.

Kallenborn, R., Gatermann, R., Nygard, T., Knutzen, J., Schlabach, M., Synthetic musks in Norwegian marine fish samples collected in the vicinity of densely populated areas. Fresenius Environ. Bull. 10, 832–842, 2001.

Lee, I.S., Lee, S.H., Oh, J.E., Occurrence and fate of synthetic musk compounds in water environment. Water Res. 44, 214–222, 2010.

Luckenbach, T., Epel, D., Nitromusk and polycyclic musk compounds as long-term inhibitors of cellular xenobiotic defense systems mediated by multi-drug transporters. Environ. Health Perspect. 113, 17–24, 2005.

Lv, Y., Yuan, T., Hu, J., Wang, W., Seasonal occurrence and behavior of synthetic musks (SMs) during wastewater treatment process in Shanghai, China. Sci. Total Environ. 408, 4170–4176, 2010.

Mack, J., Bolton, J.R., Photochemistry of nitrite and nitrate in aqueous solution: a review, J. Photochem. Photobiol. A: Chem. 128, 1–13, 1999.

Martínez-Bueno, M.J., Uclés, S., Hernando, M.D., Fernández-Alba, A.R., Development of a solvent-free method for the simultaneous identification/quantification of drugs of abuse and their metabolites in environmental water by LC–MS/MS. Talanta, 85, 157–166, 2011.

Mersch-Sundermann, V., Schneider, H., Freywald, C., Jenter, C., Parzefall, W., Knasmüller, S., Musk ketone enhances benzo(a)pyrene induced mutagenicity in human derived HepG2 cells. Mutat. Res. 495, 89–96, 2001.

Nicole, I., De Laat, J., Dore, M., Duguet, J.P., Bonnel, C., Use of UV radiation in water treatment: measurement of photonic flux by hydrogen peroxide actinometry. Water Res. 24, 157–168, 1990.

Nöthe, T., Hartmann, D., von Sonntag, J., von Sonntag, C., Fahlenkamp, H., Elimination of the musk fragrances galaxolide and tonalide from wastewater by ozonation and concomitant stripping. Water Sci Technol. 55, 287–292, 2007.

OECD, *Test No. 202: Daphnia sp. Acute Immobilisation Test*, OECD Guidelines for the Testing of Chemicals, Section 2, OECD Publishing, 2004.

OECD, Test No. 201: Freshwater Alga and Cyanobacteria, Growth Inhibition Test, OECD Guidelines for the Testing of Chemicals, Section 2, OECD Publishing, 2011.

Prieto, A., Zuloaga, O., Usobiaga, A., Etxebarria, N., Fernández,L. A., Development of a stir bar sorptive extraction and thermal desorption-gas chromatography-mass spectrometry method for the simultaneous determination of several persistent organic pollutants in water samples. J. Chromatogr. A 1174,40–49, 2007.

Reiner, J.L., Berset, J.D., Kannan, K., Mass flow of polycyclic musks in two wastewater treatment plants. Arch. Environ. Contam. Toxicol. 52, 451–457, 2007.

Reiner, J.L., Kannan, K., A survey of polycyclic musks in selected household commodities from the United States. Chemosphere 62, 867–873, 2006.

Rosal, R., Rodríguez, A., Gonzalo, M.S., García-Calvo, E., Catalytic ozonation of naproxen and carbamazepine on titanium dioxide. Appl. Catal. B: Environ. 84, 48–57, 2008a.

Rosal, R., Rodríguez, A., Perdigón-Melón, J.A., Mezcua, M., Agüera, A., Hernando, M.D., Letón, P., García-Calvo, E., Fernández-Alba, A.R., Removal of pharmaceuticals and kinetics of mineralization by O_3/H_2O_2 in a biotreated municipal wastewater, Water Res. 42, 3719–3728, 2008b.

Rosal, R., Gonzalo, M.S., Boltes, K., Letón, P., Vaquero, J.J., García-Calvo, E., Identification of intermediates and ecotoxicity assessment of the oxidation products generated during the ozonation of clofibric acid, J. Hazard. Mater. 172, 1061–1068, 2009.

Rosal, R., Rodríguez, A., Perdigón-Melón, J.A., Petre, A., García-Calvo, E., Gómez, M.J., Agüera, A., Fernández-Alba, A.R., Occurrence of emerging pollutants in urban wastewater and their removal through biological treatment followed by ozonation, Water Res. 44, 578–588, 2010a.

Rosal, R., Gonzalo, M.S., Rodríguez, A., García-Calvo, E., Catalytic ozonation of fenofibric acid over alumina-supported manganese oxide, J. Hazard. Mater. 183, 271–278, 2010b.

Rosenfeldt, E.J., Linden, K.G., Canonica, S., von Gunten, U., Comparison of the efficiency of OH radical formation during ozonation and the advanced oxidation processes O_3/H_2O_2 and UV/H_2O_2, Water Res. 40, 3695–3704, 2006.

Salvito, D., Synthetic Musk Compounds and Effects on Human Health?, Environ. Health Perspect., 113, 802–803, 2005.

Santiago, J., Agüera, A., Gómez-Ramos, M.M., Fernández Alba, A.R., García-Calvo, E., Rosal, R., Oxidation by-products and ecotoxicity assessment during the photodegradation of fenofibric acid in aqueous solution with UV and UV/H_2O_2, J. Hazard. Mater. 194, 30–41, 2011.

Schmid, P., Kohler, M., Gujer, E., Zennegg, M., Lanfranchi, M., Persistent organic pollutants, brominated flame retardants and synthetic musks in fish from remote alpine lakes in Switzerland. Chemosphere 67, S16–S21, 2007.

Seco, J.I., Fernández-Pereira, C., Vale, J., A study of the leachate toxicity of metal-containing solid wastes using Daphnia magna. Ecotoxicol. Environ. Saf. 56, 339 –350, 2003.

Sommer, C., The role of musks and musk compounds in the fragrance industry, in Gerhard G. Rimkus (Ed.) Synthetic Musk Fragrances in the Environment, The Handbook of Environmental Chemistry, Vol. 3, Part X, pp. 1–16, 2004

Ternes, T.A., Bonerz, M., Herrmann, N., Teiser, B., Andersen, H.R., Irrigation of treated wastewater in Braunschweig, Germany: An option to remove pharmaceuticals and musk fragrances. Chemosphere 66, 894–904, 2007.

Vesela, S., Vijverberg, J., Effect of body size on toxicity of zinc in neonates of four differently sized *Daphnia* species, Aquat. Ecol. 41, 67–73, 2007.

Ytreberg, E., Karlsson, J., Eklund, B., Comparison of toxicity and release rates of Cu and Zn from anti-fouling paints leached in natural and arti fi cial brackish seawater, Sci. Total Environ. 408, 2459 – 2466, 2010.